



The selective insertion of carbon dioxide into a lanthanide(III) 2,6-di-*t*-butyl-phenoxide bond

Leigh Anna M. Steele^a, Timothy J. Boyle^{a,*}, Richard A. Kemp^{a,b,*}, Curtis Moore^c

^a Sandia National Laboratories, Advanced Materials Laboratory, 1001 University Boulevard, SE, Albuquerque, NM 87106, United States

^b University of New Mexico, Department of Chemistry and Chemical Biology, 1 University of New Mexico, Albuquerque, NM 87131, United States

^c University of California, San Diego, Department of Chemistry and Biochemistry, 9500 Gilman Drive, La Jolla, CA 92093-0358, United States

ARTICLE INFO

Article history:

Received 20 February 2012

Accepted 21 May 2012

Available online 28 May 2012

Keywords:

CO₂(g) insertion
Lanthanide alkoxides
Carbonates

ABSTRACT

An investigation of the CO₂(g) insertion products for a series of fully characterized monomeric lanthanide 2,6-di-*t*-butyl-phenoxide compounds ([Ln(DBP)₃]; Ln = Ce (**1**), Sm (**2**), Dy (**3**), Y (**4**), Er (**5**), Yb (**6**), and Lu (**7**)) was undertaken at low pressure (<5 psi). From the products isolated, only one CO₂(g) molecule per molecule [Ln(DBP)₃] was found to insert, forming either the [Ce(μ_c-O₂C-DBP)(DBP)₂]₂ (**8**) or [Ln(μ-O₂C-DBP)(DBP)₂]₂ (Ln = Sm (**9**), Dy (**10**), Y (**11**), Er (**12**), Yb (**13**), and Lu (**14**)) structure. The purity of the bulk powders of **8–14** were verified by FT-IR and elemental analyses; however solution structures could not be studied due to the low solubility of the complexes. Higher pressures to increase the degree of CO₂(g) insertions did not alter the degree of substitution. The selectivity of CO₂(g) insertion was attributed to an interaction of the methyl moieties of the DBP ligand blocking coordination sites on the Ln metal center, as observed in the solid and solution state of **1–7**.

© 2012 Elsevier Ltd. All rights reserved.

1. Introduction

Lanthanide alkoxides ([Ln(OR)₃]) have become of interest for the production of ceramic materials [1] due to a number of inherent properties this family of compounds possesses. In particular, the lanthanide contraction [2] imparts a smooth and systematic change in cation size without altering the charge. This allows for fine-tuning of the properties of materials through subtle structural and electronic changes as different Ln cations are substituted. As an example, the fatigue behavior of the perovskite phase of lead zirconium titanate (PZT) materials was successfully decreased through the doping of PZT with the aliovalent Dy cation as determined from the systematic study of Ln-doped PZT with a series of [Ln(OR)₃] [3]. Further, the inherent luminescent properties of several of the Ln cations allow for their use in such diverse research arenas as bio-imaging agents (i.e., upconvert materials) that mimic naturally occurring fluorescent minerals [1a] or scintillator materials [4] for detecting radioactive materials.

The predominantly ionic bonding character that exists for [Ln(OR)₃] is due to the 'buried' *f*-orbitals that reside in lower energy levels than the outer *d*-orbitals [5]. Thus, the primarily electrostatic interactions between the large Ln cations and the

hetero-atoms of the –OR ligands result in irregular geometric arrangements and a wide range of coordination environments [6]. This phenomenon, coupled with the paramagnetic nature of a number of these compounds, typically requires crystal structure investigations in order to fully characterize the [Ln(OR)₃] precursors. Knowing the structural properties is helpful in optimizing the processing parameters for the final ceramic materials of interest. Often, the as-generated oxide material is not crystalline and requires thermal treatment to obtain the desired ceramic oxide phase. Unfortunately, as the [Ln(OR)₃] complexes are thermally treated, they often form carbonates through absorption of carbon dioxide [CO₂(g)] from circumjacent atmosphere, ligand decomposition, or both. The resultant carbonates require much higher processing temperatures to convert them into the desired oxide phase, an undesirable attribute that has limited their utility. Understanding this CO₂(g) insertion process and how to control it is of interest to reduce the thermal budget of final materials produced.

While research concerning the insertion of small molecules such as CO₂(g) into the metal-oxygen bonds of transition metal [M(OR)_{*n*}] complexes is voluminous, few studies concerning the reactivity of CO₂(g) with [Ln(OR)₃] compounds are available [7]. Furthermore, no structurally characterized lanthanide carbonate [Ln(O₂COR)₃] compounds that are derived from the insertion of CO₂(g) into Ln–OR bonds have been reported [6b,8]. Comparative studies with transition metals would not benefit in understanding this reactivity due to the covalent nature of the transition metal [M(OR)_{*n*}] species versus the more ionic nature of the [Ln(OR)₃] bonding [5].

* Corresponding authors. Tel.: +1 505 272 7625; fax: +1 505 272 7336 (T.J. Boyle), tel.: +1 505 272 7609; fax: +1 505 272 7336 (R.A. Kemp).

E-mail addresses: tjboyle@sandia.gov (T.J. Boyle), rakemp@UNM.edu (R.A. Kemp).

The focus of this research was to determine the extent and structural changes that occur from the insertion of CO₂(g) into the Ln–O bonds of [Ln(OR)₃] compounds as a means to understand the thermal conversion of these precursors into ceramic materials. To achieve this goal, a series of structurally similar [Ln(OR)₃] precursors that were coordinatively unsaturated was necessary to serve as the precursor compounds. The alcohol 2,6-di-*t*-butylphenol (2,6-[(CH₃)₃C]₂C₆H₃OH or H-DBP ligand) was selected for use, mainly due to its steric bulk and the previously known, tri-coordinated monomeric structures reported for [Ln(DBP)₃] (Ln = Ce [9], Pr [10], Nd [10], and Dy [3]). Since not all of the [Ln(DBP)₃] complexes are known as structurally characterized materials, we were interested in expanding and preparing a series of monomeric and unsolvated complexes. This was successfully achieved where Ln = Ce (1) [9], Sm (2), Dy (3) [3], Y (4), Er (5) Yb (6), and Lu (7) compounds. These cations were chosen to represent a range of the lighter and heavier Ln cations. Once characterized, the monomeric compounds 1–7 were treated with CO₂(g) to form [Ce(μ_c-O₂C-DBP)(DBP)₂]₂ (8) (‘μ_c’ denotes chelating bridging) and [Ln(μ-O₂C-DBP)(DBP)₂]₂ [Ln = Sm (9), Dy (10), Y (11), Er (12), Yb (13), and Lu (14)]. The syntheses and characterization of 1–14 will be discussed in detail.

2. Materials and methods

All compounds described below were handled with rigorous exclusion of air and water using standard Schlenk line and glove box techniques unless otherwise noted. The following reagents and solvents were used as received (Aldrich): H-DBP, LnCl₃ (Ln = Ce, Sm, Dy, Y, Er, Yb, Lu), KN(SiMe₃)₂, THF, and toluene. CO₂(g) in 99.999% purity was supplied by Trigas (8200 Washington Street Northeast, Albuquerque, NM 87113). [Ln(NR₂)₃] were synthesized from the reaction of anhydrous LnCl₃ and KN(SiMe₃)₂ and the products were characterized and found to be in agreement with the literature [11].

All analyses were performed on dry crystalline materials. FT-IR spectroscopic data were obtained using KBr pressed pellets using a Bruker Vector 22 Instrument under an atmosphere of flowing nitrogen. Elemental analyses were collected on a Perkin-Elmer 2400 CHN–S/O elemental analyzer. Solution state ¹³C{¹H} NMR spectra were obtained using a 5 mm BB solution probe on a Bruker AMX 400 MHz spectrometer. All spectra were referenced against the protons in deuterated toluene-*d*₈. Samples were made up in a glovebox using crystalline material and the sample tubes were flame sealed under vacuum to avoid reaction with the atmosphere.

2.1. [Ln(DBP)₃] syntheses

A general synthesis will be described, since the preparation of all the [Ln(DBP)₃] compounds were identical. To a stirring solution of [Ln(N(SiMe₃)₂)₃] dissolved in ~5 mL of toluene under an argon atmosphere, a solution of three equivalents of H-DBP in toluene (~5 mL) was added drop-wise. For most of the reactions a color change occurred immediately and the reaction was allowed to stir for 12 h. After this time the reaction mixture was concentrated by slow evaporation of the volatile components until X-ray quality crystals were formed. Compounds 1 [9] and 3 [3] have been published previously.

[Sm(DBP)₃] (2): Used [Sm(N(SiMe₃)₂)₃] (0.50 g, 0.79 mmol), H-DBP (0.57 g, 2.8 mmol) and ~10 mL of tol. Color changed from pale yellow to orange. Yield 0.50 g (82%). FT-IR (KBr, cm⁻¹): 3642(m), 3079(w), 2957(m), 1583(s), 1411(s), 1386(m, sh), 1358(s, sh), 1347(s), 1244(m), 1195(s), 1143(s), 1124(s), 1098(m), 869(s), 819(s), 796(s, sh), 748(s), 658(s), 564(s), 548(s), 452(s). ¹³C{¹H} NMR (100.5 MHz, C₇D₈) δ 154.2, 135.9, 120.3 (C₆H₃), 34.3 [–C(CH₃)₃], 30.3 [–C(CH₃)₃].

Anal. Calc. C₄₂H₆₃O₃Sm (MW = 766.36 g/mol): C, 65.83; H, 8.29. Found: C, 66.16; H, 8.34%.

[Y(DBP)₃] (4): Used [Y(N(SiMe₃)₂)₃] (0.50 g, 0.88 mmol), H-DBP (0.54 g, 2.6 mmol) and ~10 mL of tol. No color change was observed. Yield 0.23 g (37%). FT-IR (KBr, cm⁻¹): 3650(m), 2956(s), 2917(s,sh), 2872(w,sh), 2368(w), 2345(w), 1459(w), 1426(w,sh), 1407(s), 1384(m,sh), 1360(m,sh), 1316(m), 1240(s), 1199(m), 1123(w), 1103(m), 998(m), 925(w), 865(s), 821(s), 806(s), 795(w,sh), 751(s), 695(m), 658(s), 588(w,sh), 548(s), 527(w,sh), 450(s). ¹³C{¹H} NMR (100.5 MHz, C₇D₈) δ 154.2, 136.0, 120.3 (C₆H₃), 34.3 [–C(CH₃)₃], 30.3 [–C(CH₃)₃]. Anal. Calc. C₄₂H₆₃O₃Y (MW = 704.83 g/mol): C, 71.55; H, 9.01. Found: C, 72.15; H, 9.46%.

[Er(DBP)₃] (5): Used [Er(N(SiMe₃)₂)₃] (0.50 g, 0.77 mmol), H-DBP (0.48 g, 2.3 mmol) and ~10 mL of tol. No color change was observed. Yield 0.52 g (87%). FT-IR (KBr, cm⁻¹): 3651(s), 3081(w, sh), 2959(s), 2872(w,sh), 2369(w), 1412(s), 1387(s), 1358(m), 1315(w,m) 1260(s), 1196(m), 1098(s), 1022(m,sh), 976(m,sh), 936(w), 875(s), 820(m), 807(m), 748(s), 663(s), 607(m), 548(s), 453(s). Anal. Calc. C₄₂H₆₃O₃Er (MW = 782.74 g/mol): C, 64.41; H, 8.11. Found: C, 64.32; H, 8.99%.

[Yb(DBP)₃] (6): Used [Yb(N(SiMe₃)₂)₃] (0.50 g, 0.77 mmol), H-DBP (0.55 g, 2.7 mmol) and ~10 mL of tol. Color changed from red to dark red/brown. Yield 0.54 g (89%). FT-IR (KBr, cm⁻¹): 3648(m), 2951(m), 2362(w), 1457(s), 1246(s), 1361(m), 1315(m), 1250(w), 1231(m, sh), 1198(m), 1143(s), 1122(m), 1023(w), 868(m), 844(m), 821(s, sh), 806(m), 795(m), 747(s), 667(m), 588(m), 446(m), 419(s). ¹³C{¹H} NMR (100.5 MHz, C₇D₈) δ 154.3, 135.8, 120.3 (C₆H₃), 34.3 [–C(CH₃)₃], 30.4 [–C(CH₃)₃]. Anal. Calc. C₄₂H₆₃O₃Yb (MW = 789.00 g/mol): C, 63.94; H, 8.05. Found: C, 63.76; H, 8.52%.

[Lu(DBP)₃] (7): Used [Lu(N(SiMe₃)₂)₃] (0.50 g, 0.76 mmol), H-DBP (0.55 g, 2.7 mmol) and ~10 mL of tol. Changed from pale yellow to light purple. Yield 0.39 g (65%). FT-IR (KBr, cm⁻¹): 3645(m), 3081(w, sh), 2957(m), 1457(m), 1425(m), 1388(s, sh), 1360(s, sh), 1316(s, sh), 1250(m, sh), 1231(s), 1196(s, sh), 1143(s), 1122(s), 1095(s, sh), 1023(m), 878(s), 844(m), 821(m), 806(s, sh), 795(s), 746(s), 667(m), 588(m), 527(m), 449(m), 419(m). ¹³C{¹H} NMR (100.5 MHz, C₇D₈) δ 154.2, 135.8, 120.3 (C₆H₃), 35.0 [–C(CH₃)₃], 30.4 [–C(CH₃)₃]. Anal. Calc. C₄₂H₆₃LuO₃ (MW = 790.89 g/mol): C, 63.78; H, 8.03. Found: C, 64.21; H, 7.98%.

2.2. CO₂(g) insertion synthesis

A 53 mM solution of the appropriate precursor (1–7) dissolved in toluene was put into a two-neck round bottom reaction flask equipped with a nitrogen adaptor and a rubber septum. The flask containing the solution was carefully transferred from the glovebox to the Schlenk line and placed under an Ar atmosphere. An oil bubbler was used to ensure a positive pressure of gas was maintained in the flask. Technical grade CO₂(g) (5 psig) was purged through tubing equipped with a syringe needle for 2 min to clean the line of air and yield a positive pressure of CO₂(g). The needle was then stuck into the septum and the argon shut off so that the oil bubbler could monitor CO₂(g) flow. The solution was stirred under an atmosphere of CO₂(g) for 30 min during which no color change was observed. Some of the volatile components were removed *via* vacuum distillation and the remaining solution was transferred to the glovebox for slow evaporation crystal growth.

[Ce(DBP)₂(μ_c-O₂C-DBP)]₂ (8): Used 1 (0.60 g, 0.79 mmol) in ~15 mL toluene with no color change noted. Yield 0.20 g (32%). FT-IR (KBr, cm⁻¹): 3643(m), 2960(s), 2873(w, sh), 1625(w, sh), 1589(s), 1577(m, sh), 1482(w), 1426(s), 1411(w, sh), 1369(s), 1349(s), 1232(m, sh), 1248(s), 1195(m), 1176(m), 1143(s), 1105(s), 1039(w, sh), 1024(m), 861(s), 844(s, sh), 819(s), 807(s), 796(s), 747(s), 722(s), 676(m), 653(s), 588(m), 544(m), 450(s).

Anal. Calc. for $C_{86}H_{126}Ce_2O_{10}$ (MW = 1600.11 g/mol): C, 64.55; H, 7.94. Found: C, 64.10; H, 8.04%.

$[Sm(DBP)_2(\mu-O_2C-DBP)]_2 \cdot tol$ (**9**): Used **2** (0.61 g, 0.79 mmol) in ~15 mL toluene. Solution changed from bright yellow to a green upon $CO_2(g)$ addition. Yield 0.55 g (81%). FT-IR (KBr, cm^{-1}): 3642(m), 2962(s), 1626(s), 1589(w), 1482(w), 1413(m), 1387(m), 1370(s, sh), 1347(s), 1238(m), 1188(m), 1144(s), 1115(s), 1023(m), 867(s), 844(s, sh), 820(s), 806(s, sh), 797(s), 749(s), 715(m), 569(s), 547(m), 450(m). Anal. Calc. $C_{86}H_{126}O_{10}Sm_2$ (MW = 1620.74 g/mol w/o toluene): C, 63.73; H, 7.84. Found: C, 63.97; H, 7.86%.

$[Dy(DBP)_2(\mu-O_2C-DBP)]_2 \cdot tol$ (**10**): Used **3** (0.62 g, 0.80 mmol) in ~15 mL toluene with no color change noted. Yield 0.45 g (65%). FT-IR (KBr, cm^{-1}): 3642(m), 2961(m), 2284(w), 1619(m), 1583(s, sh), 1481(w), 1425(s), 1370(m, sh), 1348(m), 1263(m), 1231(s, sh), 1188(m), 1144(m, sh), 1117(s), 1023(w), 873(s), 844(s), 822(s), 796(s, sh), 770(s), 748(s), 694(w), 663(m), 451(w). Anal. Calc. $C_{93}H_{133}O_{10}Dy_2$ (MW = 1734.99 g/mol): C, 64.32; H, 7.73. Found: C, 64.51; H, 8.01%.

$[Y(DBP)_2(\mu-O_2C-DBP)]_2$ (**11**): Used **4** (0.62 g, 0.80 mmol) in ~15 mL toluene with no color change noted. Yield 0.53 g (71%). FT-IR (KBr, cm^{-1}): 3642(s), 3080(s), 2957(s), 2872(w,sh), 1625(s), 1561(m), 1468(w,sh), 1425(s), 1389(s), 1365(s,sh), 1315(s), 1250(s), 1230(s), 1195(s), 1169(s), 1147(s), 1122(s), 1094(s), 1023(m), 879(s), 844(s), 806(s,sh), 795(s), 749(s), 620(s), 588(s), 452(s). Anal. Calc. $C_{80}H_{126}O_{10}Y_2$ (MW = 1425.66 g/mol): C, 67.38; H, 8.91. Found: C, 67.07; H, 8.82%.

$[Er(DBP)_2(\mu-O_2C-DBP)]_2$ (**12**): Used **5** (0.62 g, 0.80 mmol) in ~15 mL toluene with no color change noted. Yield 0.35 g (46%). FT-IR (KBr, cm^{-1}): 3650(s), 3082(m,sh), 2959(s), 2874(w,sh), 2346(w), 1630(s), 1535(m), 1466(m), 1459(s), 1426(s,sh), 1413(m), 1369(s), 1347(s), 1261(s), 1231(s), 1194(s), 1143(s), 1116(s), 1094(m,sh), 1023(m), 976(m), 872(s), 844(m), 822(s,sh), 806(m), 796(m), 747(s), 710(m), 677(s), 660(m,sh), 588(m), 448(m). Anal. Calc. $C_{80}H_{126}O_{10}Er_2$ (MW = 1582.36 g/mol): C, 60.70; H, 8.03. Found: C, 60.82; H, 7.69%.

$[Yb(DBP)_2(\mu-O_2C-DBP)]_2$ (**13**): Used **6** (0.63 g, 0.80 mmol) in ~15 mL toluene with no color change noted. Yield 0.42 g (63%). FT-IR (KBr, cm^{-1}): 3650(m), 2961(m), 2874(w, sh), 2347(m), 1630(s), 1585(s, sh), 1420(s), 1388(m), 1372(s), 1353(m), 1262(m), 1246(m, sh), 1187(s, sh), 1143(m), 1118(s), 1024(m), 875(s), 844(s), 822(s), 804(s), 771(s, sh), 752(s), 718(s), 665(s), 590(m), 452(s). Anal. Calc. $C_{86}H_{126}O_{10}Yb_2$ (MW = 1665.01 g/mol): C, 61.98; H, 7.63. Found: C, 62.24; H, 7.87.

$[Lu(DBP)_2(\mu-O_2C-DBP)]_2$ (**14**): Used **7** (0.63 g, 0.80 mmol) in ~15 mL toluene with no color change noted. Yield 0.36 g (54%). FT-IR (KBr, cm^{-1}): 3648(m), 3082(w, sh), 2959(m), 2202(w), 1458(s), 1369(s, sh), 1349(m), 1316(s, sh), 1251(m, sh), 1230(s), 1194(s, sh), 1143(s), 1117(s), 1094(s, sh), 1023(m), 879(s), 844(m), 806(s, sh), 795(s), 746(s), 713(m), 678(m), 588(m), 446(m), 419(m). Anal. Calc. for $C_{86}H_{126}Lu_2O_{10}$ (MW = 1669.88 g/mol): C, 61.86; H, 7.61. Found: C, 62.32; H, 8.02%.

2.3. General X-ray crystal structure information

Single crystals were mounted onto a glass fiber from a pool of Fluorolube™ and immediately placed in a cold N_2 vapor stream, on a Bruker AXS diffractometer employing an incident-beam graphite monochromator, Mo $K\alpha$ radiation ($\lambda = 0.7107 \text{ \AA}$) and a SMART APEX CCD detector. Lattice determination and data collection were carried out using SMART Version 5.054 software. Data reduction was performed using SAINTPLUS Version 6.01 software and corrected for absorption using the SADABS program within the SAINT software package [12]. Structures were solved by direct methods that yielded the heavy atoms, along with a number of the lighter atoms or by using the PATTERSON method, which yielded the

heavy atoms. Subsequent Fourier syntheses yielded the remaining light-atom positions. The hydrogen atoms were fixed in positions of ideal geometry and refined using SHELX software [12a]. The final refinement of each compound included anisotropic thermal parameters for all non-hydrogen atoms. Table 1 lists the unit cell parameters for the structurally characterized compounds **1–14**. All final CIF files were checked using the CheckCIF program (<http://www.iucr.org/>). Additional information concerning the data collection and final structural solutions can be found by accessing CIF files through the Cambridge Crystallographic Data Base. Additional information concerning the data collection and final structural solutions can be found in the CCDC database.

2.4. Specific problems related to structures

For the structural solutions of **1–6**, the space group changes from $P21$ for Er (and all those proceeding) to $P21/c$ (for Tm and all those following) without a change in the overall structure. Disorder in the Ln centers were noted in the solutions of **1–6** [95/5% for Ce2/Ce2a; 65/45% for Y1/Y1a; 55/45% for Er1/Er2; 50/50% for Yb1/Yb2; and 52/48% for Lu1/Lu2] and were modeled appropriately. In addition, each structure presented a rotational disorder in one of the *t*-butyl groups of the DBP that was modeled appropriately. For **9** a disordered molecule of toluene was removed by the SQUEEZE method using the PLATON program [13]. Compound **10** was found to be ‘twinned’ and PLATON was used to create the HKLF5 format file that was then used for final refinement. Unresolved disorder was present in the ligands of compound **11**, which did not allow for full convergence to be reached. A higher quality data set for these crystals could not be achieved and therefore only the unit cell information is listed; however, it is of note that this structure is isostructural with **13** (based on the unit cell determination and the other characterization methods). Compound **12** was found to be a true non-merohedral twin and was refined accordingly.

3. Results and discussion

Upon insertion into a metal-ligand bond, the CO_2 moiety can act in both nucleophilic and electrophilic manners. This behavior allows for a wide range of binding environments, several of which have been crystallographically characterized for transition metals including chelating (κ), bridging (μ), and chelating bridging (μ_κ) modes. However, essentially no information is available for the $CO_2(g)$ modification of $[Ln(OR)_3]$. One report by Bochkarev et al. [7] presented a study concerning the insertion of $CO_2(g)$ into the supposed monomeric “ $Ln(OBu^t)_3$ ” ($Ln = Pr, Nd, Sm$) complex [7]. Infrared spectroscopy confirmed the presence of a C=O stretch (1580 cm^{-1}) in the product, which was reported as $[Ln(O_2COBu^t)_3]$. Since this original study, more recent crystal structures of “ $Ln(OBu^t)_3$ ” compounds have been shown to adopt a number of nuclearities including (i) tri-nuclear $\{[Ln_3(\mu_3-OBu^t)_2(\mu_2-OBu^t)_3(OBu^t)_4(HOBU^t)_2]$ ($Ln = Ce$ or Dy) or $[La_3(\mu_3-HOBU^t)_2(\mu-OBu^t)_3(OBu^t)_6]$ containing coordinated *tert*-butanol), (ii) tetra-nuclear $[Ce_4(\mu_3-OBu^t)_3(\mu-OBu^t)_4(OBu^t)_5]$, and (iii) penta-nuclear $[Ln_5(\mu_5-O)(\mu_3-OBu^t)_4(\mu-OBu^t)_4(OBu^t)_5]$ ($Ln = La, Nd$) [3,14]. Therefore, the conclusion from the Bochkarev study was compromised due to the erroneously-characterized starting materials.

Since the reaction products of $CO_2(g)$ inserted $[Ln(OR)_3]$ compounds have not been positively identified [15], we undertook the preparation and characterization of these compounds, with an emphasis necessarily placed on single crystal X-ray diffraction. The H-DBP ligand was selected since it yields monomeric $[Ln(DBP)_3]$ complexes [3,9,10], which was of interest to ensure maximum reactivity with $CO_2(g)$ [3,9]. The synthetic route (Eq.

Table 1
Data collection parameters for **1–14**.

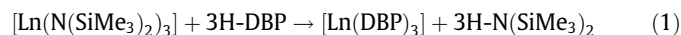
Compound	1	2	3 [3]	4	5	6	7
Formula	C ₄₂ H ₆₃ CeO ₃	C ₄₂ H ₆₃ O ₃ Sm	C ₈₄ H ₁₂₆ Dy ₂ O ₆	C ₄₂ H ₆₃ O ₃ Y	C ₄₂ H ₆₃ ErO ₃	C ₄₂ H ₆₃ O ₃ Yb	C ₄₂ H ₆₃ Lu O ₃
Formula weight	756.04	766.36	1556.85	704.83	783.18	788.96	790.89
T (K)	173(2)	173(2)	173(2)	173(2)	173(2)	173(2)	173(2)
Space group	monoclinic, P2(1)	monoclinic, P2(1)	monoclinic, P2(1)	monoclinic, P2(1)/c	monoclinic, P2(1)/c	monoclinic, P2(1)/c	monoclinic, P2(1)/c
a (Å)	11.3190(6)	11.2819(7)	11.2323(8)	11.1912(12)	11.1850(7)	11.1268(7)	11.1123(6)
b (Å)	31.7246(16)	31.781(2)	31.769(2)	31.914(4)	31.902(2)	31.959(2)	31.9676(17)
c (Å)	11.6835(6)	11.6196(7)	11.5480(8)	11.6345(13)	11.6241(8)	11.6466(7)	11.5971(6)
β (°)	105.0760(10)	105.0140(10)	104.9970(10)	104.5890(10)	104.6790(10)	104.3480(10)	104.3590(10)
V (Å ³)	4051.0(4)	4024.0(4)	3980.4(5)	4021.3(8)	4012.3(5)	4012.4(4)	3991.0(4)
Z	4	4	2	4	4	4	4
D _{calc} (Mg/m ³)	1.240	1.265	1.299	1.164	1.297	1.306	1.316
μ (Mo, Kα) (mm ⁻¹)	1.157	1.493	1.911	1.484	2.125	2.365	2.508
R ₁ ^b (%) (all data)	3.10(3.38)	3.16(3.44)	4.66(5.62)	4.61(8.12)	3.89 (6.77)	4.42(9.10)	3.94(4.76)
wR ₂ ^c (%) (all data)	7.88(8.32)	7.76(8.31)	8.40(8.87)	10.43(11.20)	10.70(13.40)	7.62(8.99)	10.82(11.61)
Compound	8	9^{tol}	10^{tol}	11^a	12^{tol}	13	14
Formula	C ₈₆ H ₁₂₆ Ce ₂ O ₁₀	C ₈₆ H ₁₂₆ O ₁₀ Sm ₂ C ₇ H ₈	C ₈₆ H ₁₂₆ Dy ₂ O ₁₀ C ₇ H ₈	C ₈₆ H ₁₂₆ O ₁₀ Y ₂	C ₈₆ H ₁₂₆ Er ₂ O ₁₀ C ₇ H ₈	C ₈₆ H ₁₂₆ O ₁₀ Yb ₂	C ₈₆ H ₁₂₆ Lu ₂ O ₁₀
Formula weight	1600.11	1712.70	1829.14	1425.66	1838.66	1665.95	1669.81
T (K)	173(2)	173(2)	173(2)	173(2)	173(2)	173(2)	173(2)
Space group	triclinic, P $\bar{1}$	monoclinic, P2(1)/c	monoclinic, P2(1)/c	monoclinic, P2(1)/n	monoclinic, P2(1)/c	monoclinic, P2(1)/n	monoclinic, P2(1)/n
a (Å)	12.470(3)	25.7656(18)	25.62(2)	14.643(8)	25.6176(18)	14.5936(17)	14.6015(12)
b (Å)	13.150(3)	17.6363(12)	17.604(17)	14.845(9)	17.6817(12)	14.8220(17)	14.8211(12)
c (Å)	13.646(3)	21.1737(14)	20.99(2)	20.195(12)	20.9385(15)	20.045(2)	20.0160(16)
α (°)	69.907(6)						
β (°)	75.781(5)	95.9760(10)	95.867(12)	108.653(12)	95.6263(11)	108.227(2)	108.0680(10)
γ (°)	76.371(5)						
V (Å ³)	2008.9(9)	9569.2(11)	9419(16)	4159(4)	9438.7(11)	4118.3(8)	4118.1(6)
Z	1	4	4	4	4	2	2
D _{calc} (Mg/m ³)	1.323	1.189	1.290	1.294	1.294	1.343	1.347
μ (Mo, Kα) (mm ⁻¹)	1.174	1.266	1.629	1.821	1.821	2.311	2.438
R ₁ ^b (%) (all data)	8.82(18.45)	4.93(7.17)	7.63(10.33)		6.13(8.05)	6.94(12.62)	5.07(9.51)
wR ₂ ^c (%) (all data)	11.72 (14.85)	15.28(16.48)	17.88 (19.50)		12.15 (13.05)	14.76(17.27)	11.85 (14.77)

^a Only the unit cell dimensions are reported due to low quality data set compound.

^b $R_1 = \frac{\sum ||F_o| - |F_c||}{\sum |F_o|} \times 100$.

^c $wR_2 = \frac{[\sum w(F_o^2 - F_c^2)^2 / \sum w(F_o^2)^2]^{1/2}}{\sum w(F_o^2)^2} \times 100$.

(1) for Ln(OR)₃ was conducted in a non-polar solvent and crystals were grown by slow evaporation. The FT-IR spectra of the products of **1–7** isolated from Eq. (1) revealed the absence of stretches attributable to the –NR₂ and –OH functionalities, indicating that the amide-alcohol exchange reaction had gone to completion [16]. To further characterize the products, the crystalline products were analyzed by single crystal X-ray diffraction.



As mentioned above, compounds **1** and **3** have been previously found to adopt a trigonal geometry around the metal center [3,9]. The refinement value for our [Ce(DBP)₃] structure is slightly lower than the previously published data and so it has been included in this report for completeness. Compounds **2**, **4**, **6** (Fig. 1), and **7** were propitiously found to adopt the same structural arrangement reported for the literature species [3,9,10]. Selected bond distances and angles are listed in Table 2 and were found to be consistent with each other and with the literature reports [3,9,10]. Upon crystallization of **5** a disordered oxo species [Er₃(μ₃-O)(μ-O)₃(HDBP)₂(DBP)₄] with cell parameters of *a*: 27.09, *b*: 13.58, *c*: 28.09, β: 91.00, *V* = 1033 Å³ was also isolated from a slow evaporation over an extended period of time; however, rapid crystallization from a more concentrated reaction system led to the desired [Er(DBP)₃] (**5**) complex. For **1–7**, the location of the Ln center was found to be disordered, which was manifested as displacement of the metal center from the plane. The observed displacements of the Ln cations are reported in the metrical data Table 2. The elemental analysis values for all of these compounds were found to be within the values suggested by the crystal structure data.

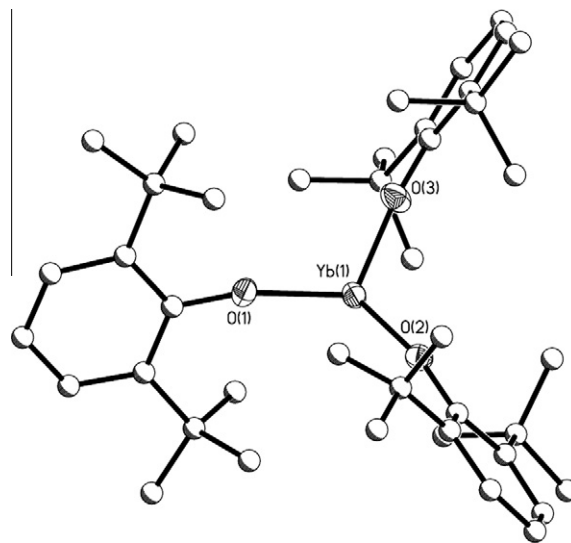


Fig. 1. The [Ln(DBP)₃] representative structure plot. Shown is [Yb(DBP)₃].

The ¹³C{¹H} NMR spectra were obtained for compounds **1–7** to analyze their solution behavior. Table 3 lists the resonances for the reference ligand H-DBP and the observed resonances for compounds **1–7** (note: the paramagnetic nature of compound **5** was too large to allow for a meaningful spectrum to be collected). For

Table 2
Metrical data for **1–14**.

Compound	Ln–OR (Å)	Ln–Ln ^a [9]	OR–Ln–OR (°)
Ce (1)	2.16	1.458	110.19
Sm (2)	2.11	1.317	109.82
Dy (3)	2.06	–	110.58
Y (4)	2.05	1.080	113.18
Er (5)	2.00	1.205	110.80
Yb (6)	2.02	0.949	113.76
Lu (7)	2.02	1.151	111.18

Compound	Ln(OR) (Å)	Ln–OCOR (Å)	OR–Ln–OR (°)	O–Ln–O (°)	O–C–O (°)
Ce (8)	2.13	2.52	233.2	Bite 49.90 Bridge 111.80	120.40
Sm (9)	2.10	2.30	108.09	96.40	120.00
Dy (10)	2.05	2.26	113.10	92.98	119.99
Y (11)	2.06	2.19	117.75	92.46	119.97
Er (12)	2.02	2.19	108.12	95.09	119.99
Yb (13)	2.02	2.16	119.10	91.80	119.95
Lu (14)	2.01	2.15	118.33	92.63	120.00

^a The displacement between the two disordered central Ln atoms.

these compounds more resonances than would be expected for the threefold D_3 symmetric $[\text{Ln}(\text{DBP})_3]$ solid state structure were observed in the *t*-butyl region. This implies either the compounds were not pure or the methyls of the DBP *t*-butyl groups were inequivalent. The former seems unlikely in that the elemental analyses of these compounds were in agreement with the expected values. Therefore, a ‘locked-out’ *t*-butyl group if persistent in solution should also be observed in the solid state. Re-examination of the solid-state structures of **1–7** did reveal that one of the methyls of the *t*-butyl groups of the DBP had a closer interaction with the Ln metal center than the others. This interaction resulted in a distance of $r_{(\text{Ln}-\text{C})}$ av. 3.1 Å. It appears that the ‘locked-out’ *t*-butyl groups (possibly occurring through H-bonding) are maintained in solution, thereby forming unique NMR environments for each methyl carbon. This was further investigated and verified by variable temperature $^{13}\text{C}\{^1\text{H}\}$ and DEPT135 NMR experiments (see Supporting Information). Combined, the NMR data confirmed the monomeric solid state structures were retained in solution with the presence of a DBP methyl–lanthanide interaction.

3.1. $\text{CO}_2(\text{g})$ insertion reactions

With this set of monomeric starting compounds (**1–7**) available, $\text{CO}_2(\text{g})$ insertion reactions were undertaken as shown in Eq. (2). The resultant products were isolated as X-ray quality crystals

Table 3
 $^{13}\text{C}\{^1\text{H}\}$ NMR chemical shifts for **1–4** and **6–7**.

Compound	δ $^{13}\text{C}\{^1\text{H}\}$: phenyl carbons ^a				$^{13}\text{C}\{^1\text{H}\}$: <i>t</i> -butyl carbons	
					–C(CH ₃) ₃	–C(CH ₃) ₃
1	<i>H</i> -DBP	155.0	135.9	125.0	120.3	34.3
	$[\text{Ce}(\text{DBP})_3]$	155.9	135.9	– ^b	120.2	37.1
2	$[\text{Sm}(\text{DBP})_3]$	154.2	138.8	–	120.3	36.2
			135.9		118.7	34.3
3	$[\text{Dy}(\text{DBP})_3]$	154.2	135.9	–	120.2	34.3
4	$[\text{Y}(\text{DBP})_3]$	154.2	137.5	–	120.3	35.4
			136.0		117.6	34.3
6	$[\text{Yb}(\text{DBP})_3]$	154.3	135.8	–	120.3	34.3
7	$[\text{Lu}(\text{DBP})_3]$	154.2	135.8	–	120.3	35.0
					118.4	30.4

^a $^{13}\text{C}\{^1\text{H}\}$ NMR shifts for **1–7**. Shifts in bold have been confirmed to be the correct assignments for each carbon by DEPT135 experiments.

^b – resonances could not be separated from the *tol-d*₈ resonances.

and ultimately proved to be a series of mono-inserted alkoxy lanthanide carbonates (**8–14**). For compound **11**, the low quality of the crystal data prevented structural convergence; however, the basic connectivity of **11** was unequivocally established and found to be in agreement with the other structures reported. The elemental analyses of the bulk powders of **8–14** were also found to be in agreement with the calculated values for the crystal structure analyses. For compounds **9**, **10**, and **12**, one loosely bound toluene solvent molecule had to be removed to obtain an acceptable analysis.



Starting DBP complex	Ln	Inserted product
1	Ce	8
2	Sm	9
3	Dy	10
4	Y	11
5	Er	12
6	Yb	13
7	Lu	14

Two structure types were observed for the $\text{CO}_2(\text{g})$ inserted products. The first type was noted for compound **8**, which was solved as a dimer with each Ce atom being 5-coordinate and adopting a distorted trigonal bipyramidal ($\tau = 0.80$) [17] geometry due to the μ_c - O_2C -DBP ligand (Fig. 2). The arrangement is dictated by the chelating/bridging ligand which causes a degree of rigidity in the final conformation. The average bond distances and angles of interest for **8** are tabulated in Table 2. This μ_c mode has been seen previously for the Ce-carbamate compound $\text{Ce}_4(\mu_4\text{-DIPC})(\mu_3\text{-DIPC})(\mu_2\text{-DIPC})_5(\mu\text{-DIPC})_2(\text{DIPC})_3$ where DIPC = *N,N'*-di-*isopropyl*carbamato) with bite, bridge, and O–C–N angles of 50.8°, 101.5°, and 120.6° respectively [18]. For compound **8** these angles were found to be similar, adopting 49.6° (bite), 111.8° (bridge), and 120.4° (O–C–O angle). There are no lanthanide carbonates that contain a bridging carbonate group; however, several transition metal species with similar carbonate ligands are available for comparison [average literature value of 119.9° (O–C–O)] [6b].

The remainder of the compounds (**9–14**) formed the same general structure motif shown in Fig. 3 (compound **13** is used as a representative compound). In this arrangement each Ln cation adopts a distorted tetrahedral (T_d) geometry using two terminal DBP and two bridging μ - O_2C -DBP ligands (Fig. 3). For **9**, **10**, and **12**, two independent molecules were found in the unit cell, and one toluene molecule was also located in the lattices of **9**, **10** and **12**. The carbonate bond angles listed in Table 2 for **9–14** are in agreement with what has been reported for carbonates found in transition metal complexes (O–C–O av. 119.9°). The change in bonding mode from **8** is associated with the size of the Ln cation.

Quite surprisingly, the products crystallized were consistent with the insertion of only one CO_2 per Ln atom. The mother liquor of the reaction mixture was not analyzed for other potential products since crystallographically identified species were of interest for this study; however, there is no inherent reason to expect only one $\text{CO}_2(\text{g})$ to insert into these $\text{Ln}(\text{DBP})_3$ complexes. To explore whether the compound could insert additional CO_2 molecules into the other remaining Ln–O bonds, elevated pressures were used to attempt to force multiple CO_2 insertions into **3**. Reactions were run under similar experimental conditions expect the $\text{CO}_2(\text{g})$ pressures were raised as high as 90 psig. Using the Dy analogue as an example, after stirring **3** with high pressure $\text{CO}_2(\text{g})$ for 30 min the colorless solution had turned dark brown and was kept at these conditions for a total of 1 h, with no further color change noticed.

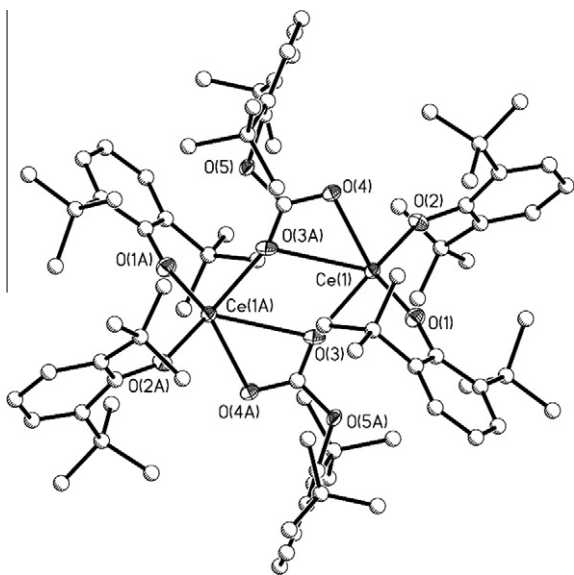


Fig. 2. Structure plot of **8**. Thermal ellipsoids of the heavy atoms are drawn at 30% level. Carbons are drawn as ball and stick for clarity.

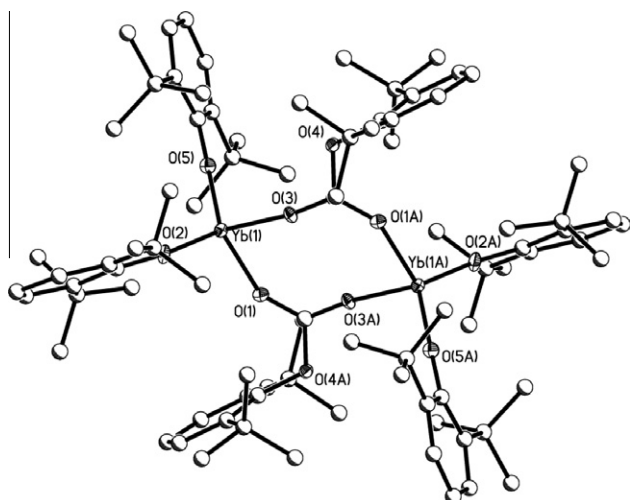


Fig. 3. Structure plot of **13**. Thermal ellipsoids of the heavy atoms are drawn at 30% level. Carbons are drawn as ball and stick for clarity.

Crystals were obtained upon slow evaporation of the solution and yielded an identical structure previously seen as **10**. This selectivity is of interest since Ln cations are known to have high coordination numbers (i.e., 7 and 8) and the final coordination geometry noted was only pseudo-Td or tbp geometry. We have preliminarily attributed this to steric encumbrance from the *t*-butyl groups' interactions with the Ln metal center, as noted in the NMR and crystal structure results (*vide infra*). These interactions may fill open sites and prevent additional CO₂(g) insertions. Further efforts with smaller and varied sterically hindering ligands are underway to explore this phenomenon and possible control the sites of multiple CO₂ insertions.

Studies were undertaken to further elucidate the carbonate binding modes. The ¹³C NMR resonance for carbonate ligands is reported to be near δ 190.0 ppm [19]. The expected slow relaxation times of Ln species, coupled with the limited solubility of the CO₂(g) insertion products (**8–14**), made obtaining useful NMR spectra difficult even with extended data collection times. Solid state NMR spectroscopy was not performed for any of the compounds

because the packing disorders that alkoxides exhibit based on restricted rotation would yield erroneous peaks and limit the amount of useful information for the compounds [14a]. FT-IR analyses indicated that the C=O stretch of –O₂COR was present as shown by a sharp band in the range of 1640–1620 cm⁻¹: **8** (1630 cm⁻¹), **9** (1626); **10** (1619), **11** (1625), **12** (1630), **13** (1630), **14** (1636). If a μ- or μ_c-O₂C bonding mode was present, a second weaker CO vibrational band in the range of 1355–1335 cm⁻¹ should be present in the IR spectra as has been observed for similar compounds with transition metals, and these bands are seen [16,20]: **8** (1346 cm⁻¹), **9** (1347), **10** (1348), **11** (1361), **12** (1347), **13** (1353), and **14** (1349). This confirms the bonding modes of the carbonate groups for **8–14** are present in the bulk powder.

4. Conclusions

The insertion of CO₂(g) into Ln–O bonds of the monomeric family of [Ln(DBP)₃] (**1–7**) compounds was found, for the first time, to form either the mono-inserted [Ce(μ_c-O₂C-DBP)(DBP)₂]₂ (**8**) or [Ln(μ-O₂C-DBP)(DBP)₂]₂ (**9–14**) species. The only substantive variation in these compounds is the bonding mode of the carbonate moiety, binding in a bridging chelate mode for the larger Ce atom in **8** and in simple bridging modes for the smaller lanthanides (**9–14**). Surprisingly, for the under-coordinated Ln metal centers only one of the three Ln–OR bonds was found to be reactive, even at higher CO₂(g) pressures. This is preliminarily attributed to the steric hindrance and *t*-butyl interaction of the DBP ligands with the Ln center reducing the number of sites for CO₂(g) to insert. Further exploration of this effort currently is underway exploring less sterically demanding ligands as well as electronically varied ligands (e.g., siloxides).

Acknowledgments

This work was supported by the Laboratory Directed Research and Development (LDRD, program 151300) program at Sandia National Laboratories and the National Science Foundation (Grant CHE09-11110 to R.A.K.). The Bruker X-ray diffractometer was purchased *via* a National Science Foundation CRIF:MU award to the University of New Mexico (CHE04-43580). Sandia National Laboratories is a multi-program laboratory managed and operated by Sandia Corporation, a wholly owned subsidiary of Lockheed Martin Corporation, for the U.S. Department of Energy's National Nuclear Security Administration under contract DE-AC04-94AL85000.

Appendix A. Supplementary data

CCDC 853343–853354 and 879692 contain the supplementary crystallographic data for **1–2**, **4–7**, and **8–14**. These data can be obtained free of charge via <http://www.ccdc.cam.ac.uk/conts/retrieving.html>, or from the Cambridge Crystallographic Data Centre, 12 Union Road, Cambridge CB2 1EZ, UK; fax: (+44) 1223-336-033; or e-mail: deposit@ccdc.cam.ac.uk. Supplementary data associated with this article can be found, in the online version, at <http://dx.doi.org/10.1016/j.poly.2012.05.021>.

References

- [1] (a) T.J. Boyle, H.D. Pratt, B.A. Hernandez-Sanchez, T.N. Lambert, T.J. Headley, *J. Mater. Sci.* 42 (2007) 2792; (b) T.J. Boyle, S.D. Bunge, N.A. Andrews, L.E. Matzen, K. Sieg, M.A. Rodriguez, T.J. Headley, *Chem. Mater.* 17 (2004) 3279.
- [2] B.E. Douglas, *J. Chem. Educ.* 31 (1954).
- [3] T.J. Boyle, S.D. Bunge, P.G. Clem, J. Richardson, J.T. Dawley, L.A.M. Ottley, M.A. Rodriguez, B.A. Tuttle, G.R. Avilucea, R.G. Tissot, *Inorg. Chem.* 44 (2005) 1588.

- [4] T.J. Boyle, L.A.M. Ottley, T.M. Alam, M.A. Rodriguez, P. Yang, S.K. McIntyre, *Polyhedron* 28 (2010) 1784.
- [5] T. Mioduski, *J. Radioanal. Nucl. Chem., Akadémiai Kiadó*, vol. 179, Co-published with Springer Science+Business Media B.V., Formerly Kluwer Academic Publishers B.V., 1993, p. 371.
- [6] (a) T.J. Boyle, L.A.M. Ottley, *Chem. Rev.* 108 (2008) 1896;
(b) CCDC ConQuest In ConQuest version 1.13 Cambridge Crystallographic Data Center: www.ccdc.cam.ac.uk, 2011 ed., vol. 2.32, 2011.
- [7] M.N. Bochkarev, E.A. Fedorova, Y.F. Rad'kov, G.S. Kalinina, S.Y. Khorshev, G.A. Razuvaev, *Dokl. Akad. Nauk. SSSR* 279 (1984) 1386.
- [8] X. Zhou, M. Zhu, *J. Organomet. Chem.* 647 (2001) 28.
- [9] H.A. Stecher, A. Sen, A.L. Rheingold, *Inorg. Chem.* 27 (1988) 1130.
- [10] H. Amberger, H. Reddmann, C. Guttenberger, B. Unrecht, L. Zhang, C. Apostolidis, O. Walter, B. Kanellakopulos, *Z. Anorg. Allg. Chem.* 629 (2003) 1522.
- [11] (a) E.D. Bradley, D.L. Clark, J.C. Gordon, P.J. Hay, W. Keogh, R. Poli, B.L. Scott, J.G. Watkin, *J. Inorg. Chem.* 42 (2003) 6682;
(b) W.A. Herrmann, R. Andwander, F.C. Munck, W. Scherer, V. Dufaud, N.W. Huber, G.R. Artus, *Z. Naturforsch. B* 49 (1994) 1789;
(c) M. Niemeyer, *Z. Anorg. Allg. Chem.* 628 (2002) 647;
(d) W.S. Rees Jr., O. Just, D.S. Van Derveer, *J. Mater. Chem.* 9 (1999) 249;
(e) G. Secarel, C. Wiemer, M. Fanciulli, I.L. Fedushkin, G.K. Fukin, G.A. Domrachev, Y. Lebedinskii, A. Zenkevich, G. Pavia, *Z. Anorg. Allg. Chem.* 633 (2007) 2097;
(f) M. Westerhausen, M. Hartmann, A. Pfitzner, W. Schwarz, *Z. Anorg. Allg. Chem.* 621 (1995) 837.
- [12] (a) G.M. Sheldrick, *Acta Crystallogr., Sect. A* A64 (2008) 112;
(b) G.M. Sheldrick, *SADABS* (2.01), Bruker/Siemens Area Detector Absorption Correction Program, Bruker AXS, Madison, Wisconsin, USA, 1998.
- [13] A.L. Spek, *J. Appl. Crystallogr.* 46 (2006) 7.
- [14] (a) T.J. Boyle, L.J. Tribby, S.D. Bunge, *Eur. J. Inorg. Chem.* (2006) 4553;
(b) D.C. Bradley, H. Chudzynska, M.B. Hursthouse, M. Motevalli, *Polyhedron* 10 (1991) 1049;
(c) S. Daniele, L.G. Hubert-Pfalzgraf, P.B. Hitchcock, M.F. Lappert, *Inorg. Chem. Commun.* 3 (2000) 218;
(d) J. Gromada, A. Mortreux, T. Chenal, J.W. Ziller, F. Leising, J.F. Carpentier, *Eur. J. Inorg. Chem.* 8 (2002) 3773.
- [15] A. Behr, *Angew. Chem., Int. Ed.* 27 (1988) 661.
- [16] G. Socrates, *Infrared and Raman Characteristic Group Frequencies: Tables and Charts*, third ed., Wiley, West Sussex, 2001.
- [17] A.W. Addison, T. Nageswara Rao, J. Reedijk, J. Van Rijn, G.C. Verschoor, *J. Chem. Soc., Dalton Trans.* (1984) 1349.
- [18] U. Baisch, D.B. Dell'Amico, F. Calderazzo, L. Labella, F. Marchetti, D. Vitali, *J. Mol. Catal. A* 204 (2003) 259.
- [19] M.G. Gardiner, N.W. Davies, A.S.P. Frey, J. Wang, *Chem. Commun.* (2006) 4853.
- [20] (a) P. Chaudhuri, V. Pavlishchuk, F. Birkelbach, T. Weyhermuller, K. Wieghardt, *Inorg. Chem.* 41 (2002) 4405;
(b) A.G. Samuelson, R. Ghosh, M. Nethaji, *Chem. Commun.* (2003) 2556;
(c) T.-B. Lu, J.-M. Chen, W. Wei, X.-L. Feng, *J. Asian Chem.* 2 (2007) 710.